Available online at www.sciencedirect.com
ScienceDirect
Catalysis Today 132 (2008) 38–45
www.elsevier.com/locate/cattod

# Acidity and catalytic activity of mesoporous ZSM-5 in comparison with zeolite ZSM-5, Al-MCM-41 and silica–alumina

K. Suzuki [a], Y. Aoyagi [a], N. Katada [a], M. Choi [b], R. Ryoo [b], M. Niwa [b,*]

[a] Department of Materials Science, Faculty of Engineering, Tottori University, Koyama, Tottori 680-8552, Japan
[b] National Creative Research Initiative Center for Functional Nanomaterials and Department of Chemistry, Korea Advanced Institute of Technology (KAIST), Daejeon 305-701, Republic of Korea

## Abstract

Acidity of mesoporous HZSM-5 prepared using amphiphilic organosilane template molecules was measured. Brønsted acid sites were observed in the prepared sample, and the number and the strength of Brønsted acid sites were determined quantitatively by a method of infrared-mass spectroscopy/temperature-programmed desorption (IRMS-TPD) of ammonia. ΔH for ammonia adsorption as an index of the strength was *ca.* 150 kJ $mol^{-1}$ that was almost the same as on usual HZSM-5, but the number was smaller than that of HZSM-5. From the measured acidity, it was concluded that the mesoporous materials contained a smaller concentration of Brønsted acid site notable on the structure of HZSM-5. Measurements of turnover frequency (TOF) in the catalytic cracking of octane supported the conclusion. Density functional calculations showed that the defect sites Al–OH and Si–OH attached to the Brønsted acid site changed the strength of the acid sites to show some possible structures of the weak and strong Brønsted acid sites included in the mesoporous HZSM-5. Acidities of Al-MCM-41 and silica–alumina were also measured, and the difference in the solid acidities of these materials was discussed.

*Keywords:* Mesoporous materials; Zeolite; ZSM-5; Acidity; IRMS-TPD; Ammonia

## 1. Introduction

Inventions of mesoporous materials by Kresge et al [1], Yanagisawa et al [2] and Inagaki et al [3] belonging to Mobil, Waseda and Toyota research groups, respectively, have led us to intensive studies for developing highly active catalytic materials. Addition of the strong acidity to these materials is anticipated, because when the strong acidity is created on the mesoporous materials, catalytic reactions of large molecules can proceed. Important studies have already been reported, in which highly active catalytic reactions have been reported over the developed catalysts [4–18].

Addition of Al atom into the MCM-41 and FSM-16, however, usually produces catalysts with relatively weak activity irrespective of the preparation methods, for example, a direct insertion of Al during the synthesis procedure or an impregnation in the post-synthesis. Some strategies [19–21] for the improvement of the solid acidity are therefore definitely required. Recently, Ryoo and coworkers reported a new method for the preparation of mesoporous material having the strong acidity [22]. They proposed to use an amphiphilic organosilane template molecule, [3-(trimethoxysilyl)propyl]-hexadecyldimethylammonium (TPHAC), and reported a successful preparation of mesoporous HZSM-5. They reported that zeolite ZSM-5 was created on the wall of the materials. Because this method is so interesting to produce the new meso- and microporous materials which have the strong acidity, in the present study, the solid acidity of synthesized mesoporous HZSM-5 is measured using an infrared-mass spectroscopy/temperature-programmed desorption (IRMS-TPD) of ammonia. This method has been recently proposed by us to overcome the difficulty of the ammonia TPD [23,24]. The Brønsted and Lewis acid sites are measured quantitatively to compare with those on usual HZSM-5, Al-MCM-41 and silica–alumina. The number and strength of the Brønsted acid sites are used as parameters to judge the presence of the ZSM-5 structure in the materials. Density functional theory (DFT) calculations will be performed in order to confirm the experimental findings,

---

* Corresponding author.
*E-mail address:* mikiniwa@chem.tottori-u.ac.jp (M. Niwa).

0920-5861/$ – see front matter © 2008 Elsevier B.V. All rights reserved.
doi:10.1016/j.cattod.2007.12.010

because the DFT calculation supported the experimentally measured ΔH (enthalpy change of ammonia adsorption) on broad kinds of zeolite species [25].

## 2. Experimental methods

### 2.1. Preparation of catalytic materials

Highly controlled mesoporous HZSM-5 was synthesized by adding TPHAC into a conventional synthesis composition of HZSM-5. The recipe to obtain a parent solution was improved in this study as follows.

### 2.2. Method 1, already reported [22]

Sodium aluminate (53 wt% $Al_2O_3$, 43 wt% $Na_2O$, Riedel-deHaën), tetra propyl ammonium bromide (TPABr) and NaOH were dissolved in distilled water. To the resultant solution, tetra ethoxy silane (TEOS or Ludox) and TPHAC (55.5 wt% methanol solution) were simultaneously added under vigorous stirring.

### 2.3. Method 2, improved to obtain higher acidity

TPHAC, TPABr and NaOH were homogeneously dissolved in $H_2O$, followed by mixing water glass solution (6.83 wt% $SiO_2$). Into the resultant homogeneous solution, a sodium aluminate solution was slowly added under stirring. Subsequently, the synthesis mixture was added with $H_2SO_4$ solution in drop wise manner under vigorous stirring conditions. The final molar composition of the gel was 2.5 $Al_2O_3$/40 $Na_2O$/95 $SiO_2$/10 TPABr/26 $H_2SO_4$/9000 $H_2O$/5 TPHAC.

### 2.4. Hydrothermal synthesis and calcination

The synthesis mixture thus prepared (Method 1 or 2) was heated with stirring at 423 K for 4 days, in a Teflon-coated stainless steel autoclave. The precipitated product was filtered by suction, and washed with distilled water. The product was dried in an oven at 373 K and subsequently calcined in air at 823 K.

A sample of HZSM-5 (KAIST) was prepared by Method 1 except for the use of TPHAC, in order to study the influence of preparation conditions on the solid acidity. One more sample of zeolite ZSM-5 (Tosoh) was kindly provided by Tosoh Co., and the molar ratio $Si/Al_2$ was 23.8.

MCM-41 was prepared according to the method reported by Ryoo and Kim [26] using $[C_{16}H_{33}N(CH_3)_3]Br$ and colloidal silica Ludox HS-40. The silica source was pre-dissolved with NaOH into an aqueous solution, prior to mixing with surfactant. The resultant gel was heated at 373 K for 24 h in a polypropylene bottle. After 24 h, pH value of the prepared gel was adjusted to 11 using a 30 wt% acetic acid solution, followed by heating again at 373 K for 24 h. The pH adjustment was repeated four times to obtain the highly synthesized mesoporous material MCM-41. After calcination at 813 K, Al was loaded from aluminum chloride on the MCM-41 by an impregnation method. The Al-loaded MCM-41 was calcined again in air at 813 K.

A commercially available catalyst (Nikki N631L) was used as a silica–alumina catalyst. The sample contained 12.5 wt% $Al_2O_3$.

### 2.5. IRMS-TPD of ammonia and catalytic cracking

Infrared spectroscopy and mass spectroscopy, connected with the glass-made vacuum apparatus, were measured simultaneously in order to follow the thermal behaviors of adsorbed and desorbed ammonia in the TPD experiment, respectively. Procedure of the experiment was described previously in detail [23]. Ammonia was adsorbed on the evacuated sample at 373 K, from which the sample temperature was elevated to 773 K. After the experiment, the difference IR spectra were calculated, and the differential change of the IR intensity with measurement temperature (hereafter called IR-TPD) was compared with MS-TPD (usual TPD) to assign the ammonia species adsorbed on Brønsted or Lewis acid site. Number of the desorbed ammonia was measured from the desorbed ammonia, and the ΔH for the adsorbed species was determined as the strength of acid site based on the theoretically derived equation for the equilibrium-controlled conditions.

Cracking of octane was measured in a Pyrex glass reactor after the pretreatment of catalyst at 773 K for 1 h. Reaction conditions were following: temperature, 773 K; partial pressure of reactant, 14 Torr (1 Torr = 133 Pa); flow rate of carrier nitrogen, 40 mL $min^{-1}$; weight of the catalyst, 30 mg. Conversion of octane was measured at 15 min after the reaction, and the reaction rate was measured under the integrated equation because the conversion often exceeded to 10%.

### 2.6. Density functional calculation for ammonia adsorption

Energy required for ammonia adsorption on the acid sites consisting of ZSM-5 framework and those modified was calculated using a software program Materials Studio $DMol^3$ developed by Accelrys Co. The geometry for initial structure of MFI zeolite was obtained from the Materials studio 4.0 library. Geometry optimizations and energy calculations of a cluster consisting of acid center in the MFI structure were carried out at generalized gradient approximations (GGA) with BLYP functional. The adsorption energy of ammonia was calculated according to the equation, $E_{ads} = E_{AS\text{-}NH3} - E_{AS} - E_{NH3}$, where $E_{ads}$ is the energy of ammonia adsorption on an acid site and $E_{AS\text{-}NH3}$, $E_{AS}$ and $E_{NH3}$ are the corresponding total energies (AS; acid site). Detail of the assumed structure is shown later.

## 3. Results

### 3.1. Measurement of acidity on mesoporous HZSM-5

Fig. 1 shows the change of IR difference spectra on the mesoporous ZSM-5 prepared by Method 1 from TEOS, which was measured during the TPD experiment; for a comparison, a

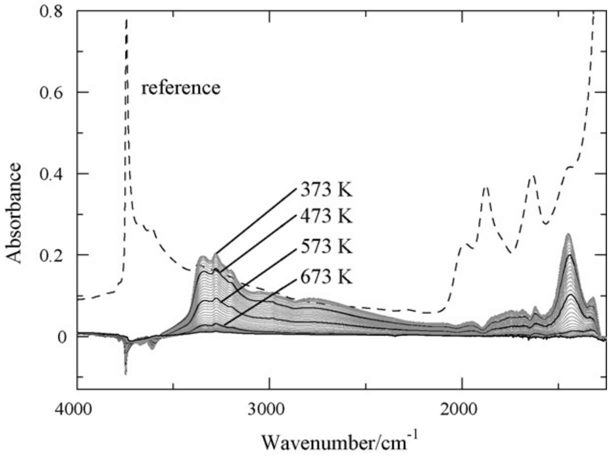

Fig. 1. Difference spectra observed upon adsorption and desorption of ammonia on the mesoporous HZSM-5 prepared by Method 1 from TEOS during the TPD experiment. Reference spectrum after the evacuation was added as a comparison.

reference IR spectrum measured after the evacuation is also shown. On adsorption of ammonia, both the stretching vibration of ammonia and the bending vibration of $NH_4^+$ and $NH_3$ were observed, while the intensities of OH bands decreased partially, showing its interaction with adsorbed ammonia species. As shown in Fig. 2(a), the bending vibration of ammonia consisted of three absorptions. A strong absorption at *ca*. 1450 $cm^{-1}$ was assigned to the bending vibration of $NH_4^+$ adsorbed species, while the bands at 1620 and 1320 $cm^{-1}$ seem to be adsorbed $NH_3$ species weakly and/or strongly adsorbed. To quantitatively measure the intensity of the absorption, a deconvolution and fitting treatment was performed, as shown in Fig. 2(b). Four portions of the absorption were assumed, and sum of the divided peaks were fitted to the experimental observation. Three of four at 1475, 1430 and 1380 $cm^{-1}$ were due to the bending vibration of $NH_4^+$, and sum of the intensities was used to calculate the change in intensity of adsorbed $NH_4^+$ with respect to the measurement temperature. Fig. 3 shows the decreased intensity of OH bands simultaneously measured during the TPD experiment. The OH absorptions that changed the intensity upon adsorption and desorption of ammonia were the IR bands observed at 3781, 3746, 3670 and 3607 $cm^{-1}$. From the band positions, these were assigned to OH on dislodged Al [27,28], isolated Si–OH, Al–OH, and the Si–O(H)–Al Brønsted acid site, respectively. The 3781-$cm^{-1}$ band of OH on the dislodged Al (Al–OH or $AlOOH^+$) was often identified in the study of β-zeolite [29], but not usually found on other species of zeolite. The difference spectra of the OH were also divided into five portions, as shown in Fig. 3(b), and the changes of these OH were calculated as mentioned above.

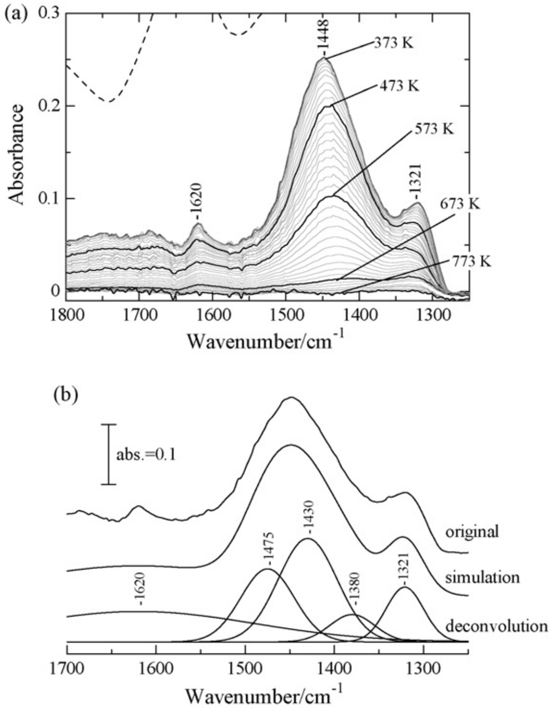

Fig. 2. (a) Magnified portion of $NH_4^+$ and $NH_3$ bending vibrations shown in Fig. 1, (b) an example of the deconvolution.

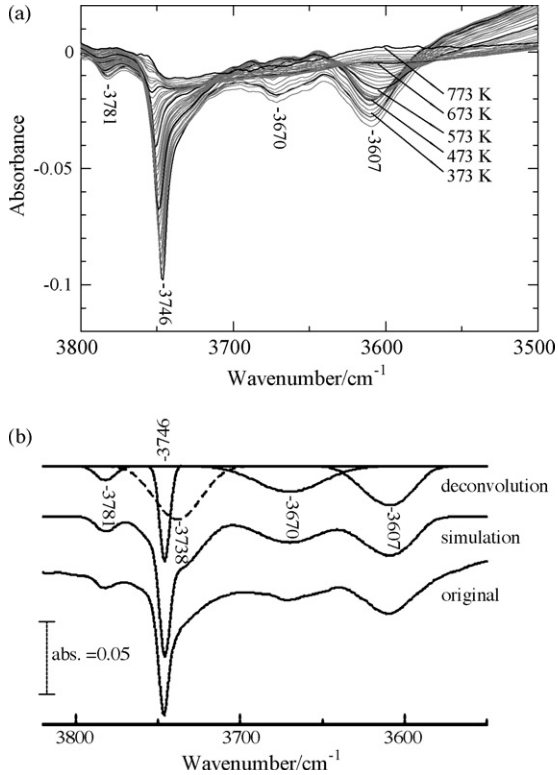

Fig. 3. (a) Magnified portion of OH stretching vibrations in Fig. 1, (b) an example of the deconvolution.

Changes of IR intensities against the measurement temperature, i.e., called IR-TPD, are shown in Fig. 4, in which MS-TPD of ammonia is shown together. MS-TPD showed two desorption peaks, while IR-TPD for ammonia and OH gave us complex profiles. From the comparison between IR- and MS-TPD profiles, following remarks were observed. From the comparison of IR-TPD for desorbed ammonia with MS-TPD, it was identified that desorption of ammonia at about 570 K mainly came from $NH_4^+$ adsorbed on the Brønsted OH. On the other hand, ammonia adsorbed as $NH_3$ was desorbed in the

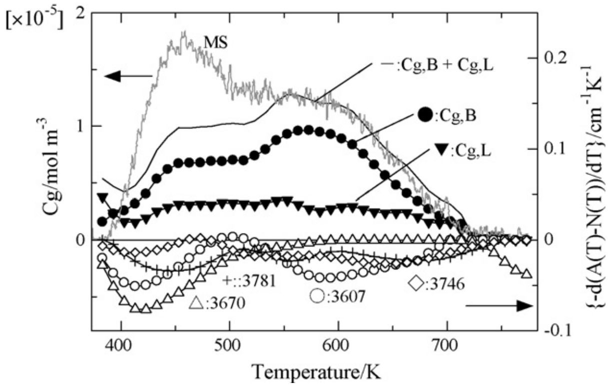

Fig. 4. IR-TPD for $NH_4^+$ and $NH_3$, and OH to be compared with MS-TPD on the mesoporous HZSM-5 prepared by Method 1 from TEOS.

broad temperature ranges from 400 to 700 K. In addition, it was found that the $NH_4^+$ band and the OH at 3607 cm$^{-1}$ changed at the same temperature regions, thus proving the Brønsted acid site. Because the $NH_4^+$ intensity changed at low temperature *ca.* 450 K also, and the Brønsted OH at 3607 cm$^{-1}$ changed its intensity at the same temperature, a small portion of ammonia was desorbed from $NH_4^+$ at the low temperature *ca.* 450 K. It was possible to identify the interaction of $NH_4^+$ with the OH at 3670 cm$^{-1}$, because the band changed the intensity at the same temperature.

The deconvolution of the TPD profile into the Brønsted and Lewis acid sites was not justified easily from the experimental finding, because both profiles strongly overlapped. Therefore, following assumptions were made for the quantitative measurements of these acid sites. Because IR bands of ammonia molecules on Brønsted and Lewis acid sites have the different extinction coefficients, the amount of desorbed ammonia is simply described as

$$\text{Amount (ammonia)} = a_1 \times I(\mathrm{NH_4}^+) + a_2 \times I(\mathrm{NH_3})$$

where $a_n$ means a parameter corresponding to reciprocal of extinction coefficient for the species and $I$ means its IR intensity. The parameters should be constants throughout the present measurements. However, in fact, constant values were not available due to the included experimental error. Therefore, in the present study, only the ratio $a_1/a_2$ was taken as nearly a constant, *ca.* 15/40. The parameter ratio being provided, number and strength of Brønsted sites were able to be calculated using a curve fitting method based on the derived theoretical equation, as shown in Table 1. However, only the number was measured for the Lewis acid site; because of the too broad profile, a distinct value of ΔH for the Lewis acid site was not determined.

Acidities on other samples of mesoporous ZSM-5 were measured using IRMS-TPD of ammonia experiments. As shown in Table 1, a sample prepared at the same synthesis conditions (Method 1) from different silica source (Ludox) had almost the same properties of number and strength of the Brønsted acid site. A sample prepared from water glass by Method 2 at the modified synthesis conditions, however, had different properties of the acidity. The $NH_4^+$ bending vibration showed the fine absorption at 1453 cm$^{-1}$, and intensities of shoulder bands at 1620 and 1320 cm$^{-1}$ were weak, as shown in Fig. 5. The Si–O(H)–Al Brønsted acid site at 3607 cm$^{-1}$ was observed distinctively in the reference spectrum, and this band decreased the intensity upon adsorption of ammonia. IRMS-TPD profiles were calculated as shown in Fig. 6 from which the number and strength of acid sites were calculated. Because the IR-TPD of the 3607-cm$^{-1}$ band had a mirror image relation with that of $NH_4^+$ bending vibration, fine Brønsted acidity was noteworthy on the mesoporous ZSM-5 (Method 2). Concentration of Brønsted acid site increased to about double as much as on meso HZSM-5 (Method 1) prepared at the initial stage of the investigation.

We speculate that the observed difference in the acidity among the mesoporous ZSM-5 samples were due to the difference in the synthesis methods. In Method 1, the aluminum source was mixed into the parent solution in vigorous conditions, while in Method 2, the aluminum source was completely dissolved into a homogeneous solution. It is speculated that the latter recipe had an advantage to disperse more Al atoms into the silicate framework to generate the Brønsted acidity.

Micro-pore volumes of the samples prepared from TEOS, Ludox, and water glass were 0.16, 0.17 and 0.17 mL g$^{-1}$, respectively. No difference in the zeolite crystal formations was therefore observed from the viewpoint of physical texture. BJH

Table 1
Solid acidity and catalytic cracking activity on mesoporous ZSM-5, usual ZSM-5, AlMCM41 and silica–alumina catalyst

| Sample (silica source, institution or company) | $Si/Al_2$ ratio | Brønsted acid (number mol kg$^{-1}$) | Brønsted acid, Strength ΔH[b] kJ mol$^{-1}$ | Lewis acid (number mol kg$^{-1}$) | Cracking rate (×10$^{-3}$ mol s$^{-1}$ kg$^{-1}$) | Turn-over frequency (×10$^{-3}$ s$^{-1}$) |
|---|---|---|---|---|---|---|
| Meso ZSM-5 (Method 1, TEOS) | 26 | 0.11 | 148 (18) | 0.04 | 2.4 | 22 |
| Meso ZSM-5 (Method 1, Ludox) | 36 | 0.13 | 148 (15) | 0.03 | 2.6 | 20 |
| Meso ZSM-5 (Method 2, water glass) | 35 | 0.3 | 151 (14) | 0.04 | 6.0 | 20 |
| ZSM-5 (KAIST) | 36 | 0.25 | 143 (6) | 0.01 | 8.3 | 33 |
| ZSM-5 (Tosoh) | 24 | 0.7 | 137 (6) | 0 | 22 | 31 |
| Al-MCM-41 | 26 | 0.14 | 130–157 | 0.15 | 0.34 | 2.4 |
| Silica–alumina (Nikki N631L) | [a] | 0.47 | 120–155 | 0.17 | 0.41 | 0.87 |

[a] 12.5 wt% $Al_2O_3$ contained.

[b] Standard deviation in the parenthesis.

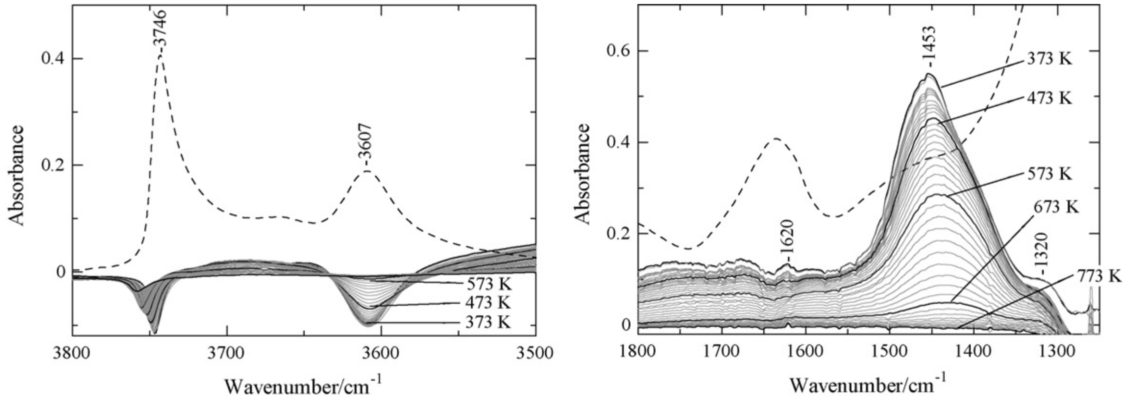

Fig. 5. Changes of difference spectra in the band positions of OH (left) and $NH_4^+$ (right) on the mesoporous HZSM-5 prepared by Method 2 from water glass.

pore diameters on these meso-pores were 11.2, 5.4 and 5.1 nm, respectively.

### 3.2. Measurement of acidity on ZSM-5, Al-MCM-41 and silica–alumina

An ordinary ZSM-5 prepared at almost the same conditions in which only the template TPHAC was excluded was measured using a method of IRMS-TPD of ammonia. As shown in Fig. 7, IR-TPD for the $NH_4^+$ adsorbed species coincided well with the MS-TPD, thus showing the predominant Brønsted acidity. Because the Brønsted OH on the sample was not clearly observed, IR-TPD for the OH was not calculated. The concentration of Brønsted acid site was larger than those of mesoporous ZSM-5 prepared at the similar conditions, meso ZSM-5 (Method 1, TEOS) and (Method 1, Ludox), as shown in Table 1. Profile of the HZSM-5 was similar to on the HZSM-5 provided by Tosoh Co. (not shown [24]); however, the latter sample had the larger concentration of Brønsted acid site.

Adsorption of ammonia on both Al-MCM-41 and silica–alumina showed both the bending vibrations of $NH_4^+$ and $NH_3$ clearly at 1437 and 1321 $cm^{-1}$, respectively. However, the Brønsted OH was not observed distinctively on these samples. IRMS-TPD for Brønsted and Lewis acid sites were calculated, as shown in Figs. 8 and 9. Both samples were characterized to be similar in the acidity as found from the IRMS-TPD, and not only the Lewis but also the Brønsted acid sites had the broad distribution of the strengths. Because of the broad distribution of the strength of the Brønsted acid sites, only the width of the $\Delta H$ was derived, as shown in Table 1.

### 3.3. Catalytic cracking of octane

To understand the catalytic property of these materials, cracking of octane was studied. The first-order reaction proceeds under the conditions of high temperature and low partial pressure, as described in the previous study by Haag and Dessau [30]. We confirmed that the reaction conditions of temperature 773 K and partial pressure of octane 14 Torr were enough to regard the reaction as proceeding under the first-order reaction mechanism [31]. In this mechanism, the penta-coordinate carbonium cation adsorbed on the Brønsted acid sites is regarded as the reaction intermediate. Therefore, the turnover frequency (TOF) was determined from the rate of the reaction and the number of the Brønsted acid site.

As shown in Table 1, the highest value of TOF was observed in two samples of ordinary HZSM-5. Compared with that on the HZSM-5, the mesoporous HZSM-5 samples showed similar values of TOF. Therefore, also from the viewpoint of catalytic

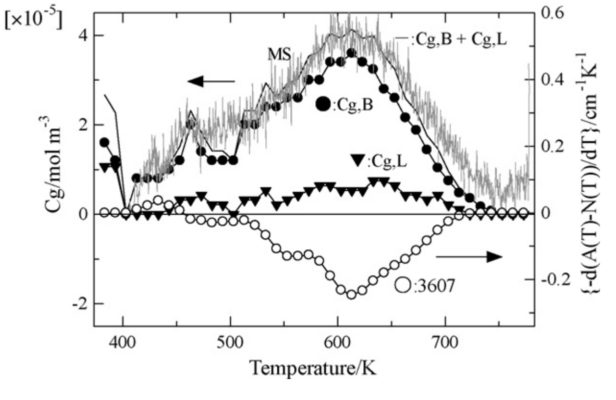

Fig. 6. IR-TPD for $NH_4^+$ (Cg, B) and $NH_3$ (Cg, L) and OH (3607) to be compared with MS-TPD on the mesoporous HZSM-5 prepared by Method 2 from water glass.

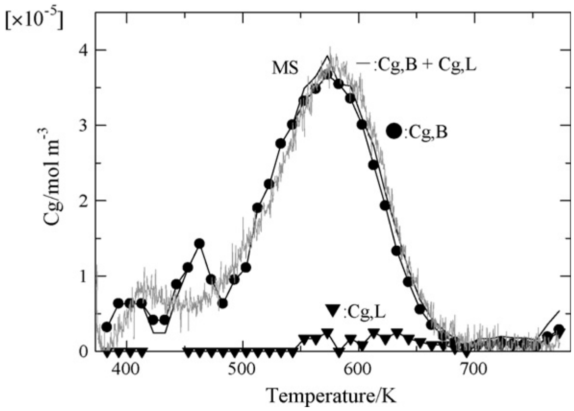

Fig. 7. IR-TPD for $NH_4^+$ (Cg, B) and $NH_3$ (Cg, L) compared with MS-TPD on the ordinary HZSM-5 (KAIST).

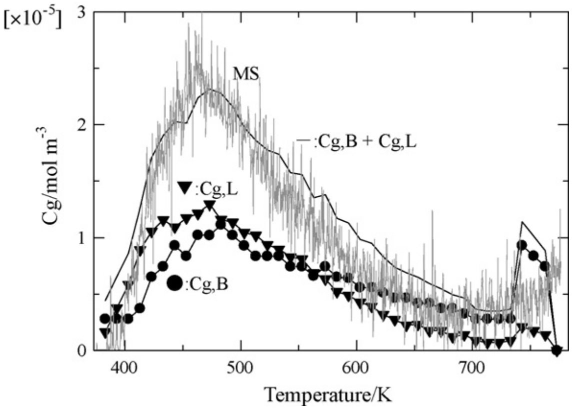

Fig. 8. IR-TPD for $NH_4^+$ (Cg, B) and $NH_3$ (Cg, L) compared with MS-TPD on the Al-MCM-41.

cracking activity, the mesoporous HZSM-5 had the property similar to the usual HZSM-5. On the other hand, Al-MCM-41 and silica–alumina showed the very small values of the TOF of the octane cracking, and it was about one tenth to one thirties of the TOF on the micro- and meso-HZSM-5.

### 3.4. Density functional calculation

Structure models of the Brønsted acid site included in the mesoporous HZSM-5 were assumed, and the Brønsted acidities were studied using a $DMol^3$ software. Table 2(a) shows the assumed structure of $NH_4^+$ from MFI zeolite. The geometry optimization was carried out for a region containing 8 T sites shown by ball and stick model, in which the T(7) site was replaced by Al, while atoms shown by wire frame were fixed at the crystallographic coordinates. The dangling silicone atom was neutralized by hydrogen, and thereby the treated cluster had a composition $NH_4AlSi_{40}O_{61}H_{42}$. Calculation for corresponding proton from cluster ($AlSi_{40}O_{61}H_{43}$) was also carried out in the same method, and the adsorption energy of ammonia was calculated. As shown in Table 2(b) and (c), adsorption energies were also calculated for other two kinds of embedded cluster models. Energy of the adsorption of ammonia on the usual HZSM-5 (model a) was 146 kJ $mol^{-1}$, and well agreed with the experimentally observed value. In the model b, $NH_4^+$ species interacts with the Si–O(H)Al–OH to show the ΔH value of 119 kJ $mol^{-1}$. In the model c, $NH_4^+$ species is stabilized on the HO–Si–O(H)–Al to show the energy of 156 kJ $mol^{-1}$. These calculated values show that the strength of ammonia adsorption changes on the acid sites attached to defect sites Al–OH or Si–OH. These are consistent with the experimental findings of IRMS-TPD, because IR-TPD for Al–OH and Si–OH changed at low and high temperatures, respectively, as shown in Fig. 4. Therefore, it is possible to estimate that these structures are included in the mesoporous HZSM-5.

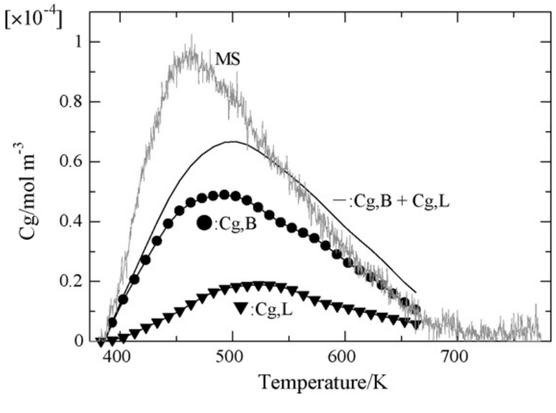

Fig. 9. IR-TPD for $NH_4^+$ (Cg, B) and $NH_3$ (Cg, L) compared with MS-TPD on the silica–alumina.

## 4. Discussion

HZSM-5 zeolite has the fine Brønsted acidity, i.e., number of the site is equal or close to number of Al located in the framework, and the strength ΔH is about 135–140 kJ $mol^{-1}$. The strength of acid site depends on the structure of zeolite as reported previously [32]; therefore, the value of the ΔH is a parameter to identify the presence of structure in the studied material. In other words, we can identify the quantity and quality of the zeolitic structure from the number and strength of the Brønsted acidity, respectively. IRMS-TPD of ammonia is a method to measure the Brønsted acid sites directly and individually. Using this method, therefore, the solid acidity of the mesoporous HZSM-5 can be studied quantitatively.

The mesoporous HZSM-5 prepared by Ryoo and coworkers has the Brønsted acidity with the ΔH of about 150 kJ $mol^{-1}$, which is a little larger than that of HZSM-5. Number of the Brønsted acid site is however less than that of the usual HZSM-5. Therefore, a simple conclusion that we can draw from the observation is a partial formation of the structure of HZSM-5 in the mesoporous materials. Presence of the structure depended on the synthesis procedure, and at most optimized preparation (Method 2), the mesoporous material includes the zeolite HZSM-5 by *ca.* 50% in compared with HZSM-5 (Tosoh).

A distribution of the Brønsted acidity was observed in the less improved samples of the mesoporous HZSM-5 (Method 1). From the profile of the TPD, a small amount of the weak Brønsted acid site was notified in addition to the usual strong Brønsted acid site. Because the Al–OH bands at 3670 and 3781 $cm^{-1}$ changed the intensity at the low temperature, it was suspected that the $NH_4^+$ species adsorbed on the Brønsted acid site interacted with these Al–OH species.

TOF for octane cracking, which was measured under the conditions of the first-order reaction, is a useful parameter to characterize the Brønsted acidity. Because of the similar values of TOF, the Brønsted acidities of the mesoporous and usual HZSM-5 resembled well. From this point of view, the presence of the HZSM-5 structure in the mesoporous HZSM-5 is clearly confirmed.

Al-MCM-41 has shown the acidity, which is similar to that on the silica–alumina catalyst. Not only the Brønsted but also the Lewis acid site is formed on the material to some degree. The IR Brønsted OH bands were not seen clearly both on silica–

Table 2
Calculated energy for ammonia adsorption on possible structure models of Brønsted acid site contained in mesoporous HZSM-5

| Model | Structure of the Brønsted acid site with adsorbed ammonium cation. In these drawings, the atoms shown by wire frame model were fixed, and those shown by ball-stick model were geometrically optimized | Energy (kJ mol$^{-1}$) |
|---|---|---|
| (a) Usual site | 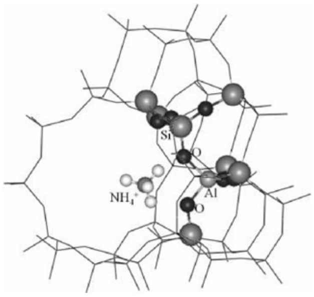 | 146 |
| (b) Site with Al–OH | 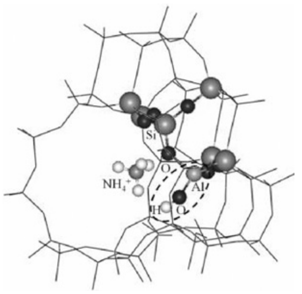 | 119 |
| (c) Site with Si–OH | 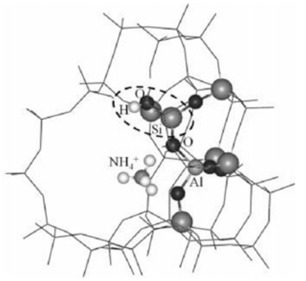 | 156 |

alumina and Al-MCM-41; however, these materials had Brønsted acidity as measured by ammonia adsorption. Numbers of these acid sites are not small compared with that on the mesoporous HZSM-5. The most striking property of the material is not the small concentration but the broad strength distribution of the acid sites. The characterized acidity implied the complex profile of the acid sites with Brønsted and Lewis characters. In other words, complex profiles of the surface structure are estimated.

Density functional calculation suggests some possible structures of Brønsted acid sites. In the present DFT study, the Al–OH in the neighbor of the Brønsted acid site decreases the strength, while the Si–OH defect site increases the strength. These calculations agree with the experimental findings, and propose a possible model of the distribution of the strength of Brønsted acid sites. The mesoporous HZSM-5 contains defects as well as the Brønsted acid site, thus showing a small distribution of the acid sites.

## 5. Conclusions

From the characterization study using IRMS-TPD of ammonia, measurements of TOF of catalytic cracking, and DFT calculation, following conclusions were obtained.

(1) From the IRMS-TPD of ammonia and TOF of catalytic cracking, it was found that the mesoporous HZSM-5 prepared using amphiphilic organosilane template molecules had the strong Brønsted acid sites notable in the HZSM-5 zeolite; but the concentration was smaller than that of HZSM-5.
(2) DFT study showed that the defect sites Al–OH and Si–OH attached to the Brønsted acid site changed the strength of the acid sites to show some possible structures of the weak and strong Brønsted acid sites included in the mesoporous materials.
(3) The Al-MCM-41 and silica–alumina were characterized to have the large distribution of acid sites and large amounts of defect sites, which differed greatly from the zeolite and mesoporous HZSM-5.

## Acknowledgment

The present work is supported by the Grant-in-Aid for Scientific Research (A) (18206082) from Ministry of Education, Culture, Sports, Science and Technology, Japan.

## References

[1] C.T. Kresge, M.E. Leonowicz, W.J. Roth, J.C. Varutuli, J.S. Beck, Nature 359 (1992) 710.
[2] T. Yanagisawa, T. Shimizu, K. Kuroda, C. Kato, Bull. Chem. Soc. Jpn. 63 (1990) 988.
[3] S. Inagaki, Y. Fukushima, K. Kuroda, J. Chem. Soc., Chem. Commun. (1993) 680.
[4] M. Busio, J. Janchen, J.H.C. van Hooff, Micropor. Mater. 5 (1995) 211.
[5] R. Mokaya, W. Jones, Z. Luan, M.D. Alba, J. Klinowski, Catal. Lett. 37 (1996) 113.
[6] J.H. Kim, M. Tanabe, M. Niwa, Micropor. Mater. 10 (1997) 85.
[7] Y. Yue, Y. Sun, Q. Xu, Z. Gao, Appl. Catal. A: Gen. 175 (1998) 131.
[8] H.H.P. Yiu, D.R. Brown, Catal. Lett. 56 (1998) 57.
[9] J. Wang, L. Huang, H. Chen, Q. Li, Catal. Lett. 55 (1998) 157.
[10] M.J. Climent, A. Corma, R. Guil-Lopez, S. Iborra, J. Primo, J. Catal. 175 (1998) 70.
[11] A. Tuel, Micropor. Mesopor. Mater. 27 (1999) 151.
[12] Y. Yue, A. Gedeon, J.-L. Bonardet, N. Melosh, J.-B. D'Espinose, J. Fraissard, Chem. Commun. (1999) 1967.
[13] L.Y. Chen, Z. Ping, G.K. Chuah, S. Jaenicke, G. Simon, Micropor. Mesopor. Mater. 27 (1999) 231.
[14] H. Kosslick, G. Lischke, B. Parlitz, W. Storek, R. Fricke, Appl. Catal. A: Gen. 184 (1999) 49.
[15] K. Chaudhari, T.K. Das, A.J. Chandwandkar, S. Sivasanker, J. Catal. 186 (1999) 81.
[16] M. Cheng, Z. Wang, K. Sakurai, F. Kumata, T. Saito, T. Komatsu, T. Yashima, Chem. Lett. (1999) 131.
[17] K. Okumura, K. Nishigaki, M. Niwa, Micropor. Mesopor. Mater. 44–45 (2001) 509.
[18] Z. Zhang, Y. Han, F.-S. Xiao, S. Qiu, L. Zhu, R. Wang, Y. Yu, Z. Zhang, B. Zou, Y. Wang, H. Sun, D. Zhao, Y. Wei, J. Am. Chem. Soc. 123 (2001) 5014.
[19] Y. Liu, W. Zhang, T. Pinnavaia, Angew. Chem. Int. Ed. 40 (2001) 1255.

[20] C.H. Christensen, K. Johannsen, I. Schmidt, C.H. Christensen, J. Am. Chem. Soc. 125 (2003) 13370.

[21] A. Ungureanu, S. Royer, T.V. Hoang, D.T. On, E. Dumitriu, S. Kaliaguine, Micropor. Mesopor. Mater. 84 (2005) 283.

[22] M. Choi, H.S. Cho, R. Srivastava, C. Venkatesan, D.-H. Choi, R. Ryoo, Nat. Mater. 5 (2006) 718.

[23] M. Niwa, K. Suzuki, N. Katada, T. Kanougi, T. Atoguchi, J. Phys. Chem. B 109 (2005) 18749.

[24] K. Suzuki, T. Noda, N. Katada, M. Niwa, J. Catal. 250 (2007) 151.

[25] K. Suzuki, G. Sastre, N. Katada, M. Niwa, Chem. Lett. 36 (2007) 1034.

[26] R. Ryoo, J.M. Kim, J. Chem. Soc., Chem. Commun. (1995) 711.

[27] E. Bourgeat-Lami, P. Massiani, F.D. Renzo, P. Espiau, F. Fajula, Appl. Catal. 72 (1991) 139.

[28] I. Kiricsi, C. Flego, G. Pazzuconi, W.O. Parker Jr., R. Millini, C. Perego, G. Bellussi, J. Phys. Chem. 98 (1994) 4627.

[29] M. Niwa, S. Nishikawa, N. Katada, Micropor. Mesopor. Mater. 82 (2005) 105.

[30] W.O. Haag, R.M. Dessau, in: Proceedings of the Eighth International Congress on Catalysis, vol. 2, Verlag Chemie, Weinheim, 1984, p. 305.

[31] T. Hashiba, D. Hayashi, N. Katada, M. Niwa, Catal. Today 97 (2004) 35.

[32] N. Katada, H. Igi, J.-H. Kim, M. Niwa, J. Phys. Chem. B 101 (1997) 5969.